Applied Physics Letters ARTICLE pubs.aip.org/aip/apl

Wigner crystallization of localized electrons in a flash memory

Cite as: Appl. Phys. Lett. **127**, 222901 (2025); doi: 10.1063/5.0288664
Submitted: 2 July 2025 · Accepted: 15 November 2025 ·
Published Online: 2 December 2025

V. A. Gritsenko,[1,2] M. M. Mahmoodian,[1,3] Mehrdad M. Mahmoodian,[1,3] A. A. Gismatulin,[1,a)] and M. V. Entin[1]

AFFILIATIONS

[1]Rzhanov Institute of Semiconductor Physics SB RAS, 13 Lavrentiev aven., 630090 Novosibirsk, Russia
[2]Novosibirsk State Technical University, 20 Marx aven., 630073 Novosibirsk, Russia
[3]Novosibirsk State University, 2 Pirogova str., Novosibirsk 630090, Russia

[a)]**Author to whom correspondence should be addressed:** aagismatulin@isp.nsc.ru

ABSTRACT

The operating principle of modern flash memory is based on the localization of electrons at dielectric traps and a subsequent change in two-dimensional semiconductor channel resistance. Amorphous silicon nitride (Si_3N_4) serves as a charge storage medium in a flash memory. In previous studies, Wigner crystallization driven by Coulomb interactions among free electrons was extensively investigated. For localized electrons, Coulomb repulsion limits the maximum charge density reachable in the dielectric. This study focuses on investigating the structural ordering, specifically Wigner crystallization, of localized electrons at deep traps (≈1.5 eV) in Si_3N_4 at room temperature. Coulomb repulsion of electrons localized at traps was experimentally observed. Experimentally, it is proven that the concentration of localized electrons is two orders of magnitude lower than that of neutral traps, indicating Coulomb repulsion between localized electrons. In this work, we investigate the structural ordering in a one-dimensional cluster of localized electrons using numerical simulations. The correlation functions of localized electrons demonstrate their Wigner crystallization. The study of Wigner ordering of localized electrons reveals that the memory properties of flash devices are governed by Coulomb interactions among these electrons rather than by the concentration of neutral traps.

Amorphous silicon nitride (Si_3N_4) has a high trap concentration and is used as a charge storage medium in modern charge trap flash memories (CTFMs).[1,2]

The higher the concentration of charged traps in Si_3N_4, the larger the memory window (difference between logical "0" and "1" states). The hypothesis of Wigner crystallization of electrons localized at traps in the dielectric is proposed in Ref. 3. It was demonstrated that electrons localized at traps in a dielectric form an ordered structure.[4]

Wigner crystallization of free electrons was theoretically predicted in 1934 by Wigner.[5] Wigner crystallization of free electrons above the surface of liquid helium was predicted in Ref. 6 and experimentally observed in Refs. 7 and 8. Wigner crystallization of charge carriers in semiconductor inversion layers was theoretically studied.[9] Experimentally, Wigner crystallization of electrons was observed in GaAs/$Al_xGa_{1-x}As$ heterostructures.[10] The one-dimensional (1D) Wigner crystallization of free electrons was observed in carbon nanotubes.[11] Two-dimensional (2D) Wigner crystals were studied in 2D free-electron gases under magnetic fields[12,13] and have been recently observed in metal dichalcogenide moiré superlattices.[14–18] Theoretically, two-dimensional Wigner crystals of free electrons were investigated,[19] including those for finite-sized systems.[20–26]

Note that neutral traps responsible for the memory effect in Si_3N_4 are randomly distributed in space. Due to Coulomb repulsion, electrons tend to be ordered, while random traps oppose ordering, forming a partly ordered structure—Wigner glass. The competition between the Coulomb interaction and disorder, arising from the random distribution of impurities, was previously studied.[27] Similar systems were investigated in the context of the Efros–Shklovskii Coulomb gap model[28,29] and vortex lattices in superconducting films.[30–34] The previously mentioned studies mostly considered Wigner crystallization at helium temperatures.

In a flash memory, electrons localize on deep traps in Si_3N_4 with the energy of 1.5 eV. When placing electrons on traps, they tend to minimize the Coulomb interaction energy. Thus, the cluster structure is determined by the minimality of Coulomb energy on the condition that electrons are randomly distributed among traps. This creates a competition between the disorder in the trap arrangement and the ordering due to Coulomb interaction. The degree of disorder is

determined by the ratio of neutral trap concentration to the electron-occupied trap concentration. Moreover, the finite cluster size leads to an influence of the total number of electrons on their ordering.[21–25]

In modern flash memory cells, the number of electrons is finite, typically in the order of 10^2–10^3, and further miniaturization is expected to reduce this number. In this paper, we experimentally determine the neutral and the charged trap concentrations. We investigate a 1D Wigner cluster (nanowire) of electrons localized at random traps and examine the effect of disorder on its properties. The study employs a numerical modeling. We will approach this problem classically. Quantum states at trap sites can be reduced to this classical problem if we neglect both the spatial state size and possible multi-charge traps.

The samples were fabricated on the n-type silicon [orientation (100)] with the resistance of 4.5 Ω × cm. Amorphous Si_3N_4 with the 66 nm thickness was deposited by the low pressure chemical vapor deposition (LPCVD) method at 700 °C from dichlorosilane SiH_2Cl_2 and ammonia NH_3 at the ratio of $SiH_2Cl_2/NH_3 = 1{:}1$. The contact was made of 350 nm thick phosphorus-doped polysilicon (poly-Si). The contact area was 6.4×10^{-3} cm^{-2}. The current–voltage characteristics (IV characteristics) were measured in a Linkam LTS420E cell using a Keythley 2400 device. The trap concentration localized in Si_3N_4 was determined by measuring the hysteresis of the capacitance–voltage (C–V) characteristics of metal–nitride–semiconductor, Si–Si_3N_4–Si_{ps}, structures using the Agilent E4980A equipment.

The expression for the occupied trap concentration in the limiting case of the uniform distribution of occupied traps over the entire dielectric thickness has the following form:

$$n_t = \frac{2C\Delta V_{FB}}{edS}. \tag{1}$$

Here, C is dielectric capacitance, ΔV_{FB} is a shift in the flatband potential during a charge accumulation, e is electron charge, d is dielectric thickness, and S is contact area.

The charge transport in Si_3N_4 is limited by the multiphonon trap ionization. At relatively low trap concentrations ($N_t \sim 10^{18}$–10^{19} cm^{-3}), a trap ionization occurs via the Makram-Ebeid model into the conduction band.[35] For high trap concentrations ($N_t \sim 10^{20}$–10^{21} cm^{-3}), the ionization proceeds through the tunneling to neighboring traps according to the Nasyrov–Gritsenko (N–G) model.[36]

The calculation of the current–voltage characteristic was performed, neglecting the space charge, using the following expression for the current density:[37]

$$J = eN_t^{2/3}P, \tag{2}$$

where P is ionization probability, and $N_t = a^{-3}$, where a is an average distance between traps.

The total concentration N_t of neutral electron traps in Si_3N_4 was determined from charge transport experiments using the N–G model. The trap ionization probability in the N–G model of phonon-assisted tunneling between neighboring traps is given by[36]

$$P = \frac{2\sqrt{\pi}\hbar W_t N_t^{2/3}}{m^*\sqrt{2kT(W_{opt}-W_t)}}\exp\left(-\frac{W_{opt}-W_t}{kT}\right) \times \exp\left(-\frac{2\sqrt{2m^*W_t}}{\hbar N_t^{1/3}}\right)\sinh\left(\frac{eF}{2kTN_t^{1/3}}\right), \tag{3}$$

where $\hbar$ is reduced Planck constant, W_t is trap thermal ionization energy, W_{opt} is optical ionization energy, m^* is electron effective mass, k is Boltzmann constant, T is temperature, and F is electric field.

The experimental and theoretical current–voltage characteristics obtained using the N–G model are presented in Fig. 1(a).

The N–G model quantitatively describes the current–voltage characteristics of the n-Si/Si_3N_4 (66 nm)/poly-Si structure with reasonable thermal and optical trap ionization energy values ($W_t = 1.5$ eV, $W_{opt} = 3.0$ eV), as shown in Fig. 1(a). The neutral trap concentration $N_t = 2.3 \times 10^{20}$ cm^{-3} was determined by fitting the experimental data to the N–G model.

The application of positive potential to the metal gate of the Si–Si_3N_4–poly-Si structure induces a positive voltage shift in the C–V characteristics indicative of the electron accumulation in the Si_3N_4 layer. The n_t dependence on ΔV_{FB} is calculated from characteristic C–V shifts. [Fig. 1(b)]. The n_t calculation was done on the assumption of a uniform distribution of occupied traps.

The experimental data revealed the occupied electron trap concentration $n_t = 1.4 \times 10^{18}$ cm^{-3} in Si_3N_4. This value is two orders of magnitude lower than the neutral trap concentration $N_t = 2.3 \times 10^{20}$ cm^{-3} determined from the charge transport measurements in Si_3N_4. This difference arises due to the Coulomb repulsion between localized electrons.

To study the influence of traps, consider the electron capture in a 1D array of deep neutral traps, with concentration N_t, containing no

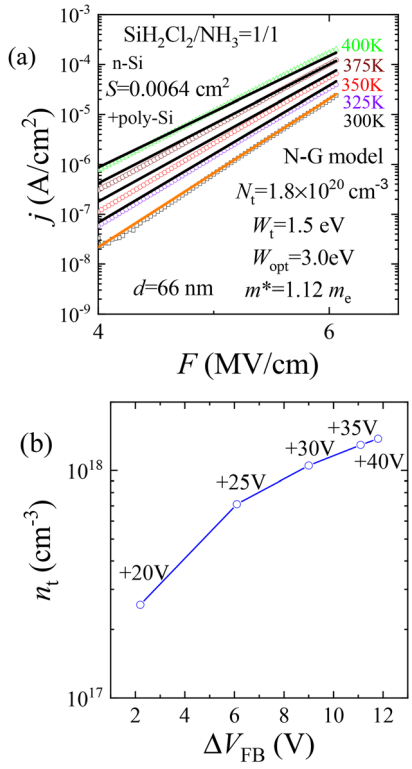

FIG. 1. (a) Current–voltage (I–V) characteristics of the n-Si/Si_3N_4(66 nm)/poly-Si structure and the theoretical curves calculated using the model of phonon-assisted tunneling between neighboring traps. (b) Concentration of charged traps vs flatband voltage shift.

free mobile charge carriers. Due to the small number of traps, electrons tend to stay at the maximal distance from each other, allowed by the trap positions, and form a disordered 1D structure—Wigner glass.

When an electron occupies a trap, it creates a repulsive potential $e^2/\varepsilon L$ for subsequent electrons, where L is the characteristic Coulomb repulsion length. A second electron with energy W_{ph} can approach an occupied trap only within a distance $2L$ determined by the relation $e^2/\varepsilon L \sim W_{ph}$. A case when a second electron approaches an electron-occupied trap is theoretically predicted in Ref. 38. In many electron systems Coulomb repulsion leads to the localized electron ordering on traps.

The occupied trap concentration $n_t \sim (2L)^{-3} = (\varepsilon W_{ph}/2e^2)^3$ does not depend on N_t. Thus, increasing N_t during the dielectric synthesis does not enhance the memory window.

Next, we consider the dielectric as a 1D system along the X axis with randomly distributed neutral traps—empty sites where electrons can be localized. Electrons are localized at random trap positions x_i, while the spatial state size is assumed to be negligible. The model excludes both multiply charged traps and free electrons since they quickly thermalize and get trapped.

Electron–electron interactions are determined by Coulomb repulsion, as well as an external parabolic potential generated by the electrode field, to compensate for electron Coulomb repulsion and keep them within the system. The parabolic potential $U(x) = \gamma x^2/2$, $(\gamma > 0)$, γ is the stiffness of the parabolic potential and x is the distance from the system center. The Coulomb interaction between electrons is described by the following expression:

$$V = \sum_{i>j} e^2/\varepsilon|x_i - x_j|, \tag{4}$$

where ε is the low-frequency dielectric permittivity of the surrounding medium, and x_i and x_j are trapped electron positions.

For numerical simulations of the system, we developed a computer program that minimizes the total system energy.

The experiment yields a neutral-to-occupied trap concentration ratio of the order of 100, which corresponds to $100^{1/3} \approx 5$ in a 1D system. Therefore, we model a 1D system with this ratio.

The electron density properties can be conveniently analyzed using the electron spatial correlation function $\xi(x)$. The function $\xi(x)$ averaged over 400 realizations of trap positions is shown in Fig. 2.

For both the free-electron system (Fig. 2, red dashed) and the high-trap-concentration system (Fig. 2, green solid), $\xi(x)$ exhibits a series of pronounced nearly equidistant peaks indicating a periodic electron ordering. The equidistant spacing breaks down at larger distances due to boundary effects. Intermediate regions show less distinct peaks resulting from a random trap distribution. This is particularly evident in the low-trap-concentration system (Fig. 2, blue solid), where the electron positioning freedom becomes severely constrained. In both the free-electron system and the system with a high trap concentration, the $\xi(x)$ functions show a good agreement while being markedly different from the low-trap-concentration case. This indicates the function's sensitivity to the electron spatial disorder.

The parabolic well is necessary to prevent electrons from escaping. However, it forces an external inhomogeneity in addition to traps. To deal with a more translational-invariant system, we consider the electrons placed on a circle. Due to the confined geometry, no confining potential is required in such a system. Note that although the considered circle is a toy system, it can be realized experimentally.

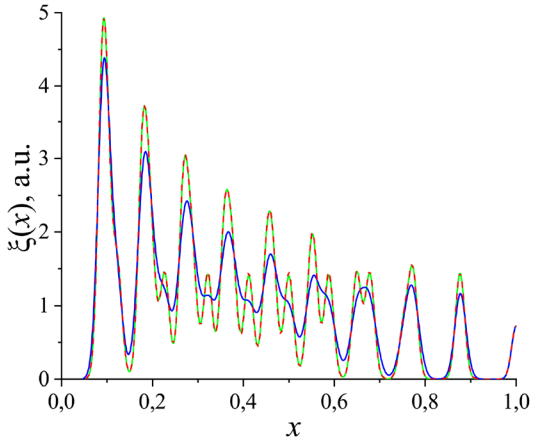

FIG. 2. Spatial correlation function $\xi(x)$ of 11 electrons for the free-electron system (red, dashed), the high-trap-concentration system (green, solid), and the low-trap-concentration system (blue, solid). x is measured in units of cluster length.

Consider randomly distributed traps on a circle. The transition from low to high electron density can be conveniently analyzed using the electron angular correlation function $\eta(\varphi)$, where φ is a polar angle. To find a correlation function of electrons, we fix one electron at the angle $\varphi = 0$ and find the positions of others.

The function $\eta(\varphi)$ averaged over 400 realizations of trap positions is shown for different trap (Fig. 3) and electron (Fig. 4) numbers. The maxima reflect the most preferable electron positions caused by the electron repulsion. When the ratio of trap and electron numbers decreases, the fluctuation in the trap positions prevails and the correlation function drops faster. The dashed lines represent envelope functions, connecting maxima of $\eta(\varphi)$.

The immanent property of the considered system is the concurrence between the Coulomb repulsion, forcing the electron ordering in a lattice (for an equidistant 1D case), and random trap positions,

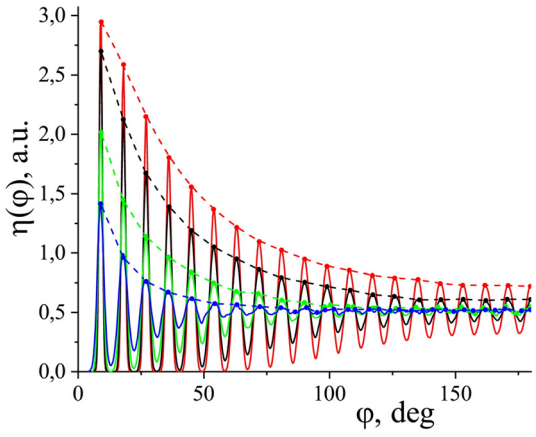

FIG. 3. Angular correlation function $\eta(\varphi)$ of 40 electrons in 200 (blue), 400 (green), and 4000 (red) random traps.

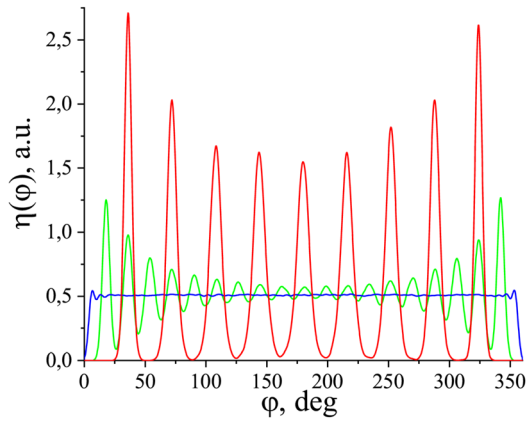

FIG. 4. Angular correlation function $\eta(\varphi)$ of 10 (red), 20 (green), and 50 electrons (blue) in the 100-random trap system.

forcing disordered electron positions. In the infinite system without traps, all electrons conserve the order over the infinite distance. The corresponding e–e correlation function does not decay at any distance. The traps induce the correlation function decay. The characteristic decay length is determined by a distance when the nearest appropriate trap occurs in half of the mean interelectron distance $l \sim 1/n_t^{1D}$, where n_t^{1D} is a 1D electron (occupied trap) concentration. That means the presence of a trap in an interval dx with the absence of traps in a box, say, $l/4 < x < 3l/4$, the probability of which is $\exp(-N_t^{1D}x)N_t^{1D}dx$. We suppose, that $n_t^{1D} \ll N_t^{1D}$, where N_t^{1D} is a 1D trap concentration. The correlation length is determined by a distance where the appropriate trap and, subsequently, the next electron get into this box,

$$\langle l_c \rangle = \int_{l/4}^{3l/4} \exp(-N_t^{1D}x)N_t^{1D}x dx \sim \frac{\exp(-N_t^{1D}/4n_t^{1D})}{4n_t^{1D}}. \quad (5)$$

The quantity $\langle l_c \rangle$ yields the correlation function decay rule $\propto \exp(-x/\langle l \rangle)$. This dependence agrees to the computer simulations.

The evolution of electron ordering with a change in electron number for the fixed trap number can be analyzed by $\eta(\varphi)$ in Fig. 4. For the highest electron number (Fig. 4, blue), $\eta(\varphi)$ is nearly constant, indicating a weakly correlated disordered state. In this regime, limited trap sites prevent the formation of long-range order, leading instead to a glassy state.

As the electron number is reduced to 20 (Fig. 4, green), a peak structure emerges in the correlation function signifying the onset of spatial ordering. However, the peaks are broad, and the central peak height is less pronounced, reflecting a system in a transitional phase where correlation effects are strengthening, but the order is not yet fully developed.

For the lowest electron number (Fig. 4, red), the Coulomb repulsion dominates and forces the electrons into a strongly correlated crystalline state. With ample traps available, the electrons localize equidistantly along the circle to minimize Coulomb energy. This results in a correlation function with distinct sharp peaks, which correspond directly to the fixed relative angles between neighboring electrons in this ordered Wigner-crystal-like arrangement. The system undergoes a clear transition from a disordered glassy state at a high density to a strongly correlated crystalline state at a low density.

In conclusion, this work experimentally demonstrates the Coulomb repulsion between localized electrons in amorphous silicon nitride (Si_3N_4), which manifested itself through the significantly lower concentration of trapped electrons (n_t), compared to neutral traps (N_t). Numerical simulations of localized electrons in a 1D model reveal the formation of Wigner clusters exhibiting their short-range order across several nearest neighbors. Unlike Wigner crystals of free electrons, the trap-localized electrons in the dielectric form a disordered nonperiodic lattice, characteristic of the Wigner glass phase, where their long-range periodicity is disrupted while maintaining the short-range order.

While Wigner crystals of free electrons are formed only at low temperatures (typically a few Kelvin), the deep traps (≈1.5 eV) in Si_3N_4 enable a Wigner glass formation by localized electrons even at high room temperature conditions.

Coulomb repulsion between localized electrons in Si_3N_4—the charge-trapping layer of CTFMs—leads to the incomplete trap filling. This effect fundamentally limits the reachable concentration of charged traps, thereby restricting the memory window in flash memory devices.

The present work was supported by the Russian Science Foundation (Grant No. 25-12-00022). The electrophysical measurements were made on the equipment of Core Facilities VTAN in the ATRC Department of the Novosibirsk State University.

AUTHOR DECLARATIONS

Conflict of Interest

The authors have no conflicts to disclose.

Author Contributions

V. A. Gritsenko: Conceptualization (equal); Funding acquisition (equal); Project administration (equal); Resources (equal); Supervision (equal); Validation (equal); Visualization (equal); Writing – original draft (equal); Writing – review & editing (equal). **M. M. Mahmoodian:** Data curation (equal); Formal analysis (equal); Investigation (equal); Methodology (equal); Software (equal); Validation (equal); Visualization (equal); Writing – original draft (equal); Writing – review & editing (equal). **Mehrdad M. Mahmoodian:** Data curation (equal); Formal analysis (equal); Investigation (equal); Software (equal); Validation (equal); Visualization (equal); Writing – original draft (equal); Writing – review & editing (equal). **A. A. Gismatulin:** Data curation (equal); Formal analysis (equal); Investigation (equal); Methodology (equal); Software (equal); Validation (equal); Visualization (equal); Writing – original draft (equal); Writing – review & editing (equal). **M. V. Entin:** Conceptualization (equal); Formal analysis (equal); Supervision (equal); Validation (equal); Writing – original draft (equal); Writing – review & editing (equal).

DATA AVAILABILITY

The data that support the findings of this study are available from the corresponding author upon reasonable request.

REFERENCES

[1]V. A. Gritsenko, *Silicon Nitride on Si: Electronic Structure for Flash Memory Devices* (World Scientific Press, 2016), Chap. VI, pp. 273–322.
[2]A. Goda, "Recent progress on 3D NAND flash technologies," Electronics **10**, 3156 (2021).
[3]V. A. Gritsenko, "Wigner crystallization and a resonance exchange mechanism for electrons localized in an amorphous insulator with a high trap density," J. Exp. Theor. Phys. Lett. **64**, 525–530 (1996).
[4]S. S. Shaimeev, V. A. Gritsenko, and H. Wong, "Wigner crystallization due to electrons localized at deep traps in two-dimensional amorphous dielectric," Appl. Phys. Lett. **96**, 263510 (2010).
[5]E. Wigner, "On the interaction of electrons in metals," Phys. Rev. **46**, 1002–1011 (1934).
[6]H. M. Van Horn, "Instability and melting of the electron solid," Phys. Rev. **157**, 342–349 (1967).
[7]R. S. Crandall and R. Williams, "Crystallization of electrons on the surface of liquid helium," Phys. Lett. A **34**, 404–405 (1971).
[8]C. Grimes and G. Adams, "Evidence for a liquid-to-crystal phase transition in a classical, two-dimensional sheet of electrons," Phys. Rev. Lett. **42**, 795–798 (1979).
[9]A. V. Chaplik, "Possible crystallization of charge carriers in low-density inversion layers," Sov. Phys. JETP **35**, 395 (1972).
[10]E. Y. Andrei, G. Deville, D. C. Glattli, F. I. B. Williams, E. Paris, and B. Etienne, "Observation of a magnetically induced Wigner solid," Phys. Rev. Lett. **60**, 2765–2768 (1988).
[11]V. V. Deshpande and M. Bockrath, "The one-dimensional Wigner crystal in carbon nanotubes," Nat. Phys. **4**, 314–318 (2008).
[12]V. J. Goldman, M. Santos, M. Shayegan, and J. E. Cunningham, "Evidence for two-dimentional quantum Wigner crystal," Phys. Rev. Lett. **65**, 2189–2192 (1990).
[13]H. Zhou, H. Polshyn, T. Taniguchi, K. Watanabe, and A. F. Young, "Solids of quantum Hall skyrmions in graphene," Nat. Phys. **16**, 154–158 (2020).
[14]H. Li, S. Li, E. C. Regan, D. Wang, W. Zhao, S. Kahn, K. Yumigeta, M. Blei, T. Taniguchi, K. Watanabe, S. Tongay, A. Zettl, M. F. Crommie, and F. Wang, "Imaging two-dimensional generalized Wigner crystals," Nature **597**, 650–654 (2021).
[15]E. C. Regan, D. Wang, C. Jin, M. I. B. Utama, B. Gao, X. Wei, S. Zhao, W. Zhao, Z. Zhang, K. Yumigeta, M. Blei, J. D. Carlström, K. Watanabe, T. Taniguchi, S. Tongay, M. Crommie, A. Zettl, and F. Wang, "Mott and generalized Wigner crystal states in WSe_2/WS_2 moire superlattices," Nature **579**, 359–363 (2020).
[16]Y. Xu, S. Liu, D. A. Rhodes, K. Watanabe, T. Taniguchi, J. Hone, V. Elser, K. F. Mak, and J. Shan, "Correlated insulating states at fractional fillings of moire superlattices," Nature **587**, 214–218 (2020).
[17]X. Huang, T. Wang, S. Miao, C. Wang, Z. Li, Z. Lian, T. Taniguchi, K. Watanabe, S. Okamoto, D. Xiao, S.-F. Shi, and Y.-T. Cui, "Correlated insulating states at fractional fillings of the WS_2/WSe_2 moire lattice," Nat. Phys. **17**, 715–719 (2021).
[18]H. Li, Z. Xiang, A. P. Reddy, T. Devakul, R. Sailus, R. Banerjee, T. Taniguchi, K. Watanabe, S. Tongay, A. Zettl, L. Fu, M. F. Crommie, and F. Wang, "Wigner molecular crystals from multielectron moiré artificial atoms," Science **385**, 86–91 (2024).
[19]M. Mazars, "The melting of the classical two-dimensional Wigner crystal," Europhys. Lett. **110**, 26003 (2015).
[20]C. Yannouleas and U. Landman, "Spontaneous symmetry breaking in single and molecular quantum dots," Phys. Rev. Lett. **82**, 5325 (1999).
[21]R. Egger, W. Häusler, C. H. Mak, and H. Grabert, "Crossover from fermi liquid to Wigner molecule behavior in quantum dots," Phys. Rev. Lett. **82**, 3320 (1999).
[22]V. M. Bedanov and F. M. Peeters, "Ordering and phase transitions of charged particles in a classical finite two-dimensional system," Phys. Rev. B **49**, 2667 (1994), and references therein.
[23]V. A. Schweigert and F. M. Peeters, "Spectral properties of classical two-dimensional clusters," Phys. Rev. B **51**, 7700 (1995).
[24]M. M. Mahmoodian, M. M. Mahmoodian, and M. V. Entin, "Theory of a two-dimensional rotating wigner cluster," JETP Lett. **115**(10), 608–614 (2022).
[25]M. M. Mahmoodian and M. V. Entin, "Theory of electron states in two-dimensional Wigner clusters," J. Phys.: Conf. Ser. **2227**, 012012 (2022).
[26]M. M. Mahmoodian, M. M. Mahmoodian, and M. V. Entin, "Spin structure and spin magnetic susceptibility of two-dimensional Wigner clusters," Phys. Solid State **65**(10), 1694–1700 (2023).
[27]R. Chitra, T. Giamarchi, and P. Le Doussal, "Pinned Wigner crystals," Phys. Rev. B **65**, 035312 (2001).
[28]A. L. Efros and B. I. Shklovskii, "Coulomb gap and low temperature conductivity of disordered systems," J. Phys. C: Solid State Phys. **8**(4), L49 (1975).
[29]A. L. Efros, "Coulomb gap in disordered systems," J. Phys. C: Solid State Phys. **9**, 2021 (1976).
[30]I. Poboiko and M. V. Feigel'man, "Two-dimensional coulomb glass as a model for vortex pinning in superconducting films," Jetp Lett. **112**(4), 234–240 (2020).
[31]B. Sacépé, M. Feigel'man, and T. M. Klapwijk, "Quantum breakdown of superconductivity in low-dimensional materials," Nat. Phys. **16**, 734–746 (2020).
[32]H. Brandt, "Elastic energy of the vortex state in type II superconductors. I. High inductions," J. Low Temp. Phys. **26**, 709–733 (1977).
[33]G. Blatter, M. V. Feigel'man, V. B. Geshkenbein, A. I. Larkin, and V. M. Vinokur, "Vortices in high-temperature superconductors," Rev. Mod. Phys. **66**, 1125 (1994).
[34]W.-K. Kwok, U. Welp, A. Glatz, A. E. Koshelev, K. J. Kihlstrom, and G. W. Crabtree, "Vortices in high-performance high-temperature superconductors," Rep. Prog. Phys. **79**, 116501 (2016).
[35]S. S. Makram-Ebeid and M. Lannoo, "Quantum model for phonon-assisted tunnel ionization of deep levels in a semiconductor," Phys. Rev. B **25**, 6406 (1982).
[36]K. A. Nasyrov and V. A. Gritsenko, "Charge transport in dielectrics via tunneling between traps," J. Appl. Phys. **109**, 097705 (2011).
[37]A. A. Gismatulin, Y. N. Novikov, N. V. Andreeva, D. S. Mazing, and V. A. Gritsenko, "Origin of exponentially large increase in the leakage current in alumina films depending on the ALD synthesis temperature," Appl. Phys. Lett. **125**(6), 062901 (2024).
[38]A. I. Shames, V. A. Gritsenko, R. I. Samoilova, Y. D. Tzvetkov, L. S. Braginsky, and M. Roger, "EPR-study of nitrogen implanted silicon nitride," Solid State Commun. **118**, 129–134 (2001).